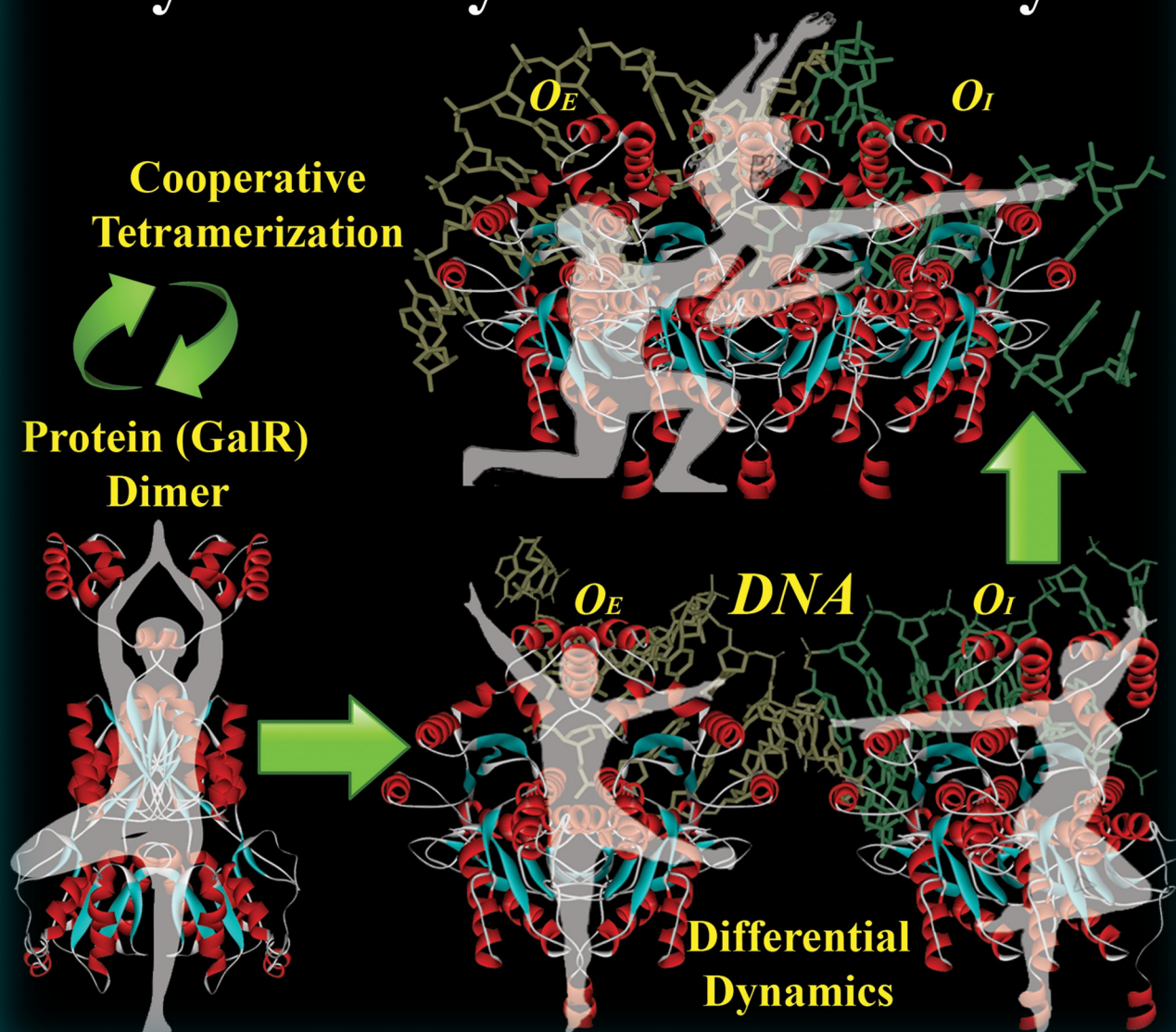


A EUROPEAN JOURNAL OF CHEMICAL BIOLOGY

# CHEM **BIO** CHEM

SYNTHETIC BIOLOGY & BIO-NANOTECHNOLOGY

## Dynamically Driven Allostery



7/2016

Cover Picture:

*P. Lemmens, S. K. Pal et al.*

Modulation of Ultrafast Conformational Dynamics in Allosteric Interaction of Gal Repressor Protein with Different Operator DNA Sequences

A Journal of



WILEY-VCH

[www.chembiochem.org](http://www.chembiochem.org)



# Modulation of Ultrafast Conformational Dynamics in Allosteric Interaction of Gal Repressor Protein with Different Operator DNA Sequences

Susobhan Choudhury,<sup>[a]</sup> Gitashri Naiya,<sup>[b]</sup> Priya Singh,<sup>[a]</sup> Peter Lemmens,<sup>\*,[c]</sup> Siddhartha Roy,<sup>[b]</sup> and Samir Kumar Pal<sup>\*,[a]</sup>

Although all forms of dynamical behaviour of a protein under allosteric interaction with effectors are predicted, little evidence of ultrafast dynamics in the interaction has been reported. Here, we demonstrate the efficacy of a combined approach involving picosecond-resolved FRET and polarisation-gated fluorescence for the exploration of ultrafast dynamics in the allosteric interaction of the Gal repressor (GalR) protein dimer with DNA operator sequences  $O_E$  and  $O_I$ . FRET from the single tryptophan residue to a covalently attached probe IAEDANS at a cysteine residue in the C-terminal domain of GalR shows structural perturbation and conformational dynamics during al-

losteric interaction. Polarisation-gated fluorescence spectroscopy of IAEDANS and another probe (FITC) covalently attached to the operator directly revealed the essential dynamics for cooperativity in the protein–protein interaction. The ultrafast resonance energy transfer from IAEDANS in the protein to FITC also revealed different dynamic flexibility in the allosteric interaction. An attempt was made to correlate the dynamic changes in the protein dimers with  $O_E$  and  $O_I$  with the consequent protein–protein interaction (tetramerisation) to form a DNA loop encompassing the promoter segment.

## Introduction

The dynamic nature of proteins and the implications for function are increasingly being appreciated.<sup>[1]</sup> The native state is now considered as a collection of energetically low-lying states with distinct conformations and dynamics, with rapid interconversion between them. These distinct states have detectable motions on many timescales, including sub-nanosecond.<sup>[2]</sup> However, little is known about their functional significance. One protein phenomenon that is definitely affected by protein dynamics, is allostery.<sup>[3,4]</sup> Allosteric regulation of proteins by binding of effector molecule/macromolecules at a site other than active site is a powerful mechanistic pathway to explain complex biochemical reactions, following the seminal work of Monod and other investigators.<sup>[5–7]</sup> Although traditional models of allostery involve significant conformational changes, there is increasing evidence that allostery can mediate solely internal protein dynamics, without significant conformational

changes.<sup>[8–12]</sup> An early seminal work by Cooper and Dryden clearly demonstrated that the effect arises out of possible changes in both high-frequency anharmonic and low-frequency highly correlated motions of individual atoms in response to the effector binding.<sup>[13]</sup> In reality, effector-induced changes to both the mean conformation and dynamics are to be expected.<sup>[14–16]</sup>

Transcription factors form a notable class of proteins where allostery plays an important role. Allostery in transcription factors is mostly known for small molecules that induces change in transcription regulatory properties of transcription factors.<sup>[17]</sup> A few cases have been reported in which the DNA sequence itself plays the role of an allosteric ligand and changes the functional outcome in terms of gene regulation.<sup>[18]</sup> However, little is known about the role of dynamics in such situations.

Because transcription factors bind to a large number of sequences in the genome and affect the final outcome in a sequence-dependent manner, we decided to explore how two distinct DNA binding sequences affect protein dynamics. We used the *Escherichia coli* galactose repressor (GalR) as a model protein and its two operator target sequences  $O_E$  and  $O_I$  as effectors.  $O_E$  is immediately upstream to two promoters P1 and P2 of the gal operon;  $O_I$  is 114 bp from  $O_E$  and is in fact located inside the first structural gene, GalE.<sup>[19]</sup> GalR, like other DNA-binding proteins, possesses a helix-turn-helix motif<sup>[20]</sup> and represses transcription upon binding to the two operator sites,  $O_E$  and  $O_I$ .<sup>[19,21]</sup> A useful feature of the repressor protein is that it is in the class of single-tryptophan-residue-containing protein has a single tryptophan residue (Trp165), and thus offers an excellent opportunity for the spectroscopic investigation of

[a] S. Choudhury, P. Singh, Prof. S. K. Pal  
Department of Chemical, Biological & Macromolecular Sciences  
S. N. Bose National Centre for Basic Sciences  
Block JD, Sector III, Salt Lake, Kolkata 700 098 (India)  
E-mail: skpal@bose.res.in

[b] G. Naiya, Prof. S. Roy  
Division of Structural Biology and Bioinformatics  
Indian Institute of Chemical Biology  
4, Raja S.C. Mullick Road, Kolkata 700 032 (India)

[c] Prof. P. Lemmens  
Institute for Condensed Matter Physics and Laboratory for Emerging  
Nanometrology  
TU Braunschweig  
Mendelssohnstrasse 3, 38106 Braunschweig (Germany)  
E-mail: p.Lemmens@tu-bs.de

this intrinsic tryptophan probe. Much evidence suggests that the binding of the repressor protein to the target DNA sequences is as a dimer.<sup>[18,22,23]</sup> Although high-resolution X-ray crystallographic/NMR structures of GalR and its complexes are not available, the protein is concluded to be similar in structure and function to another repressor protein, the Lac repressor.<sup>[24–26]</sup> We constructed a homology model of GalR by using the I-TASSER server.<sup>[27]</sup> It is very likely that binding of the GalR dimer to the DNA operators ( $O_E$  and  $O_I$ ) facilitates conformational and dynamical changes thereby leading to allosteric interactions involving additional protein–protein or protein–DNA interactions for the tetramerisation of DNA-bound GalR dimers to form a DNA loop.<sup>[25,28]</sup>

We used the single tryptophan (Trp165) of the GalR dimer as intrinsic fluorescent probe. Polarisation-gated fluorescence spectroscopy of Trp165 reveals changes in local fluctuations of the protein upon interaction with operator DNAs. FRET to a covalently labelled, cysteine-reactive extrinsic probe IAEDANS (5-(((2-Iodoacetyl)amino)ethyl)amino)naphthalene-1-sulfonic acid) at the C terminus explored intra-protein dynamics of the protein and its complexes. Polarisation-gated picoseconds-resolved fluorescence studies of IAEDANS were performed to observe the significant structural rearrangement in the C-terminal domain (active site) of the repressor protein upon protein–DNA complexation (effector site). In order to confirm the location of the IAEDANS and structural differences between GalR– $O_E/O_I$  complexes, we used FRET from IAEDANS (donor) to the acceptor FITC (fluorescein-5-isothiocyanate) attached to the operator DNA, which is bound to N-terminal domain of the GalR. The distribution of the donor–acceptor distances in the protein–DNA complexes clearly revealed changes in overall protein dynamics upon interaction with the different operators. Our results provide a clear idea of the structural and dynamic changes in GalR upon recognition of different DNA sequences. This is crucial for a deeper understanding of protein dynamics in allosteric-driven protein–protein interactions in the formation of a DNA loop.

## Results and Discussion

The steady-state emission spectra of Trp165 in GalR dimer and of IAEDANS-labelled GalR are shown in Figure 1A. The excitation spectrum of IAEDANS bound to GalR has a large overlap with the emission spectrum of Trp165 in unlabelled GalR (inset of Figure 1B; overlap integral value,  $4.22 \times 10^{14} \text{ M}^{-1} \text{ cm}^{-1} \text{ nm}^4$ ), thus indicating a high likelihood of serving as a good donor–acceptor (D–A) pair. The decrease in steady-state fluorescence of Trp165 in IAEDANS-labelled GalR relative to that of unlabelled GalR reveals an energy transfer from Trp165 to the IAEDANS through dipole–dipole coupling. Picosecond-resolved fluorescence transients of Trp165 at 350 nm ( $\lambda_{\text{ex}} = 283 \text{ nm}$ ) in native GalR and IAEDANS-labelled GalR (Figure 1B) reveal a significantly faster component of 110 ps (33%) in the time-resolved fluorescence decay of Trp165 for IAEDANS-labelled GalR compared to native GalR. The average lifetime of Trp165 decreased from 2.30 ns in GalR to 1.15 ns in IAEDANS-labelled repressor (Table 1). The energy-transfer efficiency was calculated

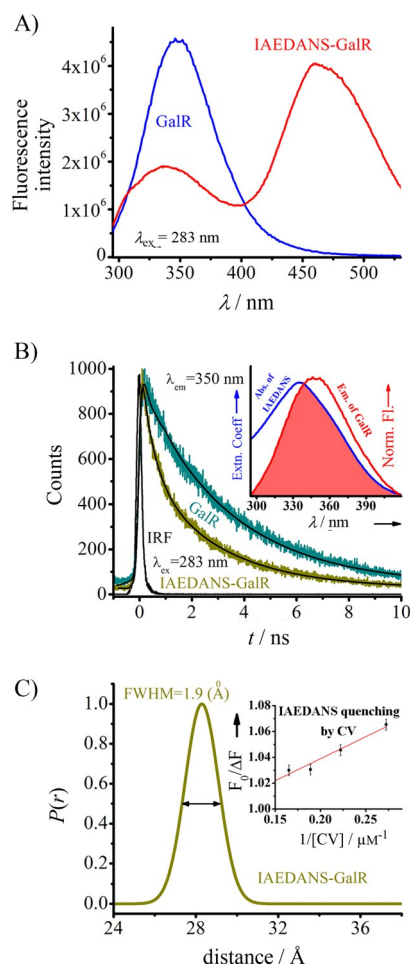


**Figure 1.** A) Steady state emission spectra of Trp165 in GalR and IAEDANS-labelled GalR ( $\lambda_{\text{ex}} = 283 \text{ nm}$ ). B) Picosecond-resolved fluorescence transients of Trp165 in GalR or IAEDANS–GalR. Inset: overlap spectra of Trp165 emission and IAEDANS absorption. C) Distribution of donor–acceptor distances in labelled GalR. Inset: modified Stern–Volmer plot for IAEDANS quenching for different concentrations of Crystal Violet. Straight line (0.5% error) yields intercept 0.97.  $F_0$  is the initial fluorescence and  $\Delta F = F_0 - \text{observed fluorescence}$  at a particular quencher concentration.

to be 50% (see the Experimental Section); as a consequence, both the calculated Förster distance ( $R_0$ ) and the Trp165–IAEDANS distance are the same (28.3  $\text{\AA}$ ). A homology model of GalR generated by I-TASSER<sup>[27]</sup> (Figure 2; tryptophan and cysteine residues highlighted) revealed that the distance between Cys155 and Trp165 is 26.33  $\text{\AA}$ . Our experimental observation of Trp165–IAEDANS distance of 28.3  $\text{\AA}$  indicates that IAEDANS is attached to Cys155 (Figure 2), thus ruling out the possibility of inter-protein FRET. The distribution of donor–acceptor distances in the labelled protein (Figure 1C) reveals internal fluctuation of the native protein<sup>[29]</sup> (no interaction with operator DNA), with a full-width half maximum (FWHM) of 1.9  $\text{\AA}$ . In order to investigate heterogeneity in the IAEDANS labelling to cysteine residues in GalR, we performed a fluorescence quenching experiment<sup>[30,31]</sup> with crystal violet (CV) as the fluorescence quencher of IAEDANS (excited state energy transfer from IAEDANS to CV). We obtained a series of steady-state emission spectra of IAEDANS-labelled GalR with increasing con-

**Table 1.** Fluorescence lifetimes ( $\tau$ ) of tryptophan residue in different systems.  $\lambda_{\text{ex}}=280$  nm,  $\lambda_{\text{em}}=350$  nm.

System	$\tau_1$		$\tau_2$		$\tau_3$		$\tau_{\text{avg}}$ [ns]
	[ps]	[%]	[ns]	[%]	[ns]	[%]	
GalR	280	33	3.33	67	–	–	2.30
GalR-IAEDANS	110	33	0.49	33	2.79	34	1.15
GalR-O <sub>E</sub>	220	40	3.06	60	–	–	1.92
O <sub>E</sub> -GalR-IAEDANS	70	85	2.20	15	–	–	0.39
GalR-O <sub>I</sub>	190	45	2.32	53	–	–	1.36
O <sub>I</sub> -GalR-IAEDANS	70	87	2.23	13	–	–	0.28

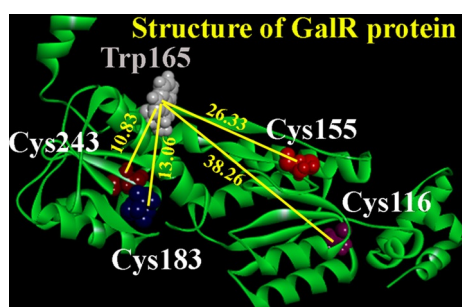


**Figure 2.** Homology model of GalR showing the distances [Å] between the tryptophan and cysteine residues.

centrations of CV, and the modified Stern–Volmer plot of  $F_0/\Delta F$  against  $1/[CV]$  (Figure 1C, inset) reveals a intercept of 0.97 upon linear fitting of the experimental data. This indicates that 97% of the fluorescence of IAEDANS is explicitly from one type of environment, consistent with the fact that the probe is attached to, essentially, one cysteine residue (Cys155).

In order to study protein dynamics alterations of GalR upon recognition of DNA sequences O<sub>E</sub> and O<sub>I</sub>, we studied FRET of unlabelled and IAEDANS-labelled GalR bound to O<sub>E</sub> or O<sub>I</sub> (Figure 3A and B, respectively). A 70 ps component for both O<sub>E</sub> and O<sub>I</sub> reflects efficient energy transfer from tryptophan to IAEDANS, and might be a consequence of crucial rearrangement of protein conformation in the C-terminal domain to bring Trp165 and IAEDANS in close proximity, in both cases (Table 1). The calculated Trp165–IAEDANS distance for GalR–O<sub>E</sub> and GalR–O<sub>I</sub> were 20.5 and 20.7 Å, respectively, and  $R_0$  values were 28.3 Å for both systems. A calculation of the distribution of donor–acceptor distances in operator-bound IAEDANS-labelled protein (Figure 3C) revealed less broadening in the case of operator-bound GalR compared to native GalR. Although O<sub>E</sub> and O<sub>I</sub> bound to GalR with similar affinities, there was a small difference in distance distribution for the two complexes: the domain fluctuation was slightly less in the O<sub>I</sub> complex (FWHM = 1.1 Å) than in the O<sub>E</sub> complex (FWHM = 1.2 Å). Actually, DNA binding (to protein) “repairs” the packing defect of tightly packed protein, thus leading to global protein fluctuation with associated entropy loss.<sup>[32,33]</sup> In principle, the entropic contribution includes changes both in internal conformational entropy and in translational and rotational entropy.<sup>[34–36]</sup> Early simulations<sup>[37]</sup> and experimental studies<sup>[38]</sup> indicated that protein domain fluctuation can reflect significant conformational entropy of the residues.

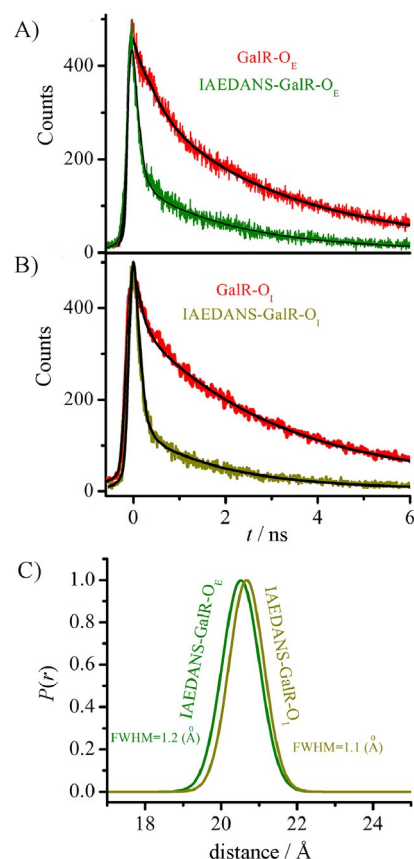


**Figure 3.** Picosecond-resolved fluorescence transients of Trp165 in unlabelled and labelled GalR in presence of A) O<sub>E</sub> or B) O<sub>I</sub>;  $\lambda_{\text{ex}}=283$  nm,  $\lambda_{\text{em}}=350$  nm. C) Distribution of donor–acceptor distances in complexes with O<sub>E</sub> and O<sub>I</sub>.

For confirmation of the structural fluctuation of GalR upon interaction with operator DNA, we performed steady-state and dynamic studies of IAEDANS attached to Cys155 (in the C-terminal domain of GalR). The emission spectra of IAEDANS (Figure 4A) show a slight blue shift in the O<sub>E</sub>/O<sub>I</sub>-GalR complexes ( $\lambda_{\text{max}}=457$  nm at  $\lambda_{\text{ex}}=375$  nm) compared to the probe in native GalR ( $\lambda_{\text{max}}=461$  nm), thus confirming shifting of the probe towards the less polar environment of the dimer protein.<sup>[39]</sup> The insignificant difference between the O<sub>E</sub>-GalR and O<sub>I</sub>-GalR complexes is consistent with the fact that the immediate environment of IAEDANS is similar in both the complexes. The emission transients of IAEDANS in native GalR and O<sub>E</sub>/O<sub>I</sub>-bound (Figure 4B;  $\lambda_{\text{ex}}=375$  nm;  $\lambda_{\text{em}}=460$  nm) show that the decay in the GalR–O<sub>I</sub> complex (90 ps, 42%) was faster than for GalR–O<sub>E</sub> (260 ps, 30%; Table 2), similarly to the tryptophan transients at 350 nm (Table 1). The faster decay of IAEDANS in the presence of O<sub>E</sub>/O<sub>I</sub> clearly reveals structural fluctuations in the C-terminal domain of GalR. Different excited-state dynamics of IAEDANS at the C-terminal of GalR upon interaction with the two operator DNAs are evident. It has to be noted that the shorter excited-state lifetime with O<sub>I</sub> than O<sub>E</sub> could also be due to excited-state electron-transfer dynamics,<sup>[40]</sup> which are also significantly different for recognition by the two operators.

In order to study rotational flexibility of the native and operator-bound protein, we investigated polarisation-gated fluores-

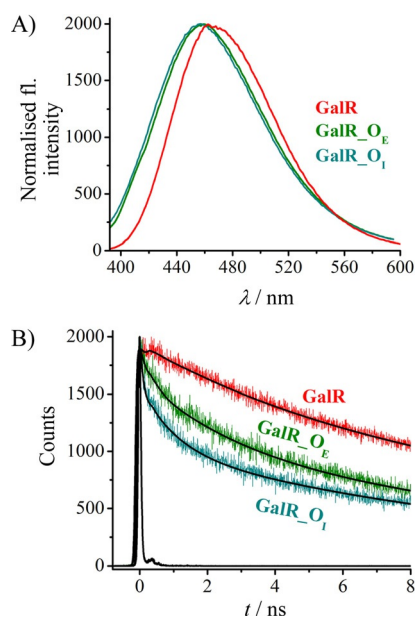


**Figure 4.** A) Steady-state emission spectra of IAEDANS-GalR alone or bound to  $O_E$  or  $O_I$ . B) Equivalent fluorescence transients.  $\lambda_{ex}=375$  nm,  $\lambda_{em}=460$  nm for all plots.

Table 2. Fluorescence lifetimes ( $\tau_i$ ) of IAEDANS attached to a cysteine residue in different systems. $\lambda_{ex}=375$ nm $\lambda_{em}=460$ nm.							
System	$\tau_1$		$\tau_2$		$\tau_3$		$\tau_{avg}$ [ns]
	[ps]	[%]	[ns]	[%]	[ns]	[%]	
IAEDANS-GalR	–	–	1.63	16	15.42	84	13.21
IAEDANS-GalR- $O_E$	260	30	2.80	27	15.90	43	7.70
IAEDANS-GalR- $O_I$	90	42	1.00	21	12.50	37	4.80

cence of IAEDANS in GalR, in the absence and presence of  $O_E$  or  $O_I$  (Figure 5). Fitting of the fluorescence anisotropy data with a multi-exponential decay function revealed 100 ps (9%), 1.0 ns (13%) and 30 ns (78%). The first two are attributable to

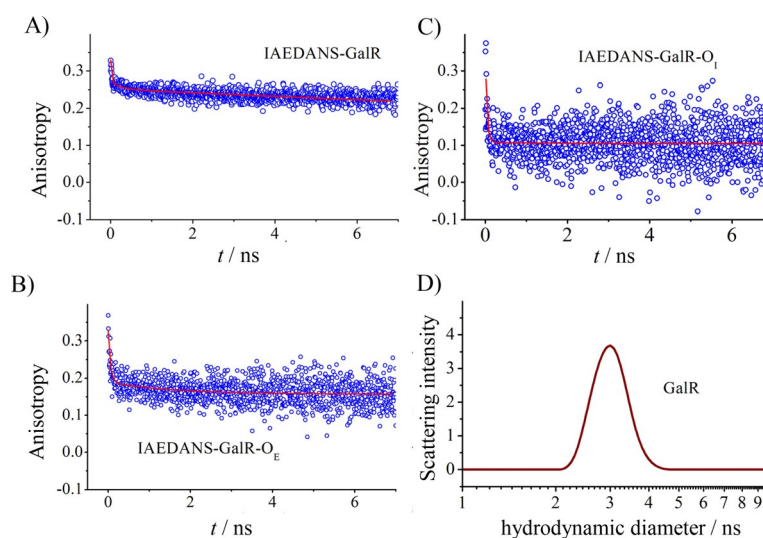


**Figure 5.** Fluorescence anisotropy of IAEDANS-GalR A) alone, B) complexed with  $O_E$ , and C) complexed with  $O_I$ . D) Typical DLS signals (scattering intensity) for GalR.  $\lambda_{ex}=375$  nm and  $\lambda_{em}=460$  nm (for plots A, B and C).

local motion of the probe, whereas the 30 ns component is consistent with a global tumbling.<sup>[18]</sup> We fixed the longer time constant (30 ns) during the fitting. Local motion of the probe is reflected by the time constants of 50 ps (37%) and 200 ps (20%) upon complexation with  $O_E$  (Table 3). However, in the case of  $O_I$ , local motion merged to a single value, 50 ps.

**Table 3.** Rotational time scales of IAEDANS attached to a cysteine residue in different systems.  $\lambda_{ex}=375$  nm  $\lambda_{em}=460$  nm.

System	$\tau_1$		$\tau_2$		$\tau_3$	
	[ps]	[%]	[ns]	[%]	[ns]	[%]
IAEDANS-GalR	100	9	1.0	13	30.0	78
IAEDANS-GalR- $O_E$	50	37	0.20	20	30.0	43
IAEDANS-GalR- $O_I$	50	58	30.0	42	–	–

This observation clearly indicates that, upon complexation with  $O_I$ , the flexibility of IAEDANS (bound to cysteine in the C-terminal domain of GalR) is much higher than for  $O_E$  (Figure 5). It is worth mentioning that the broader domain fluctuation (measured Trp165-IAEDANS FRET distance distribution) in the case of the GalR- $O_E$  complex is not a consequence of local motion of the energy acceptor (IAEDANS), as the local motion is slower than for GalR- $O_I$ . The local motion of the energy donor (Trp165) was unaltered upon complexation with  $O_E$  or  $O_I$ . Although domain fluctuation was higher for the  $O_E$  complex, due to larger contribution of conformation entropy, the particular residue fluctuation (higher in the case of the  $O_I$  complex) could be due to the rotational entropy contribution.<sup>[34,41]</sup> Both fluctuations are crucial in the case of allosteric signalling with GalR for higher-order protein-protein interaction (tetramerisation) through loop formation, as deletion/substitution of either  $O_E$  or  $O_I$  rendered GalR ineffective in repression.<sup>[21]</sup>

For investigation of the location of the IAEDANS-bound cysteine with respect to the operator DNA, we performed FRET

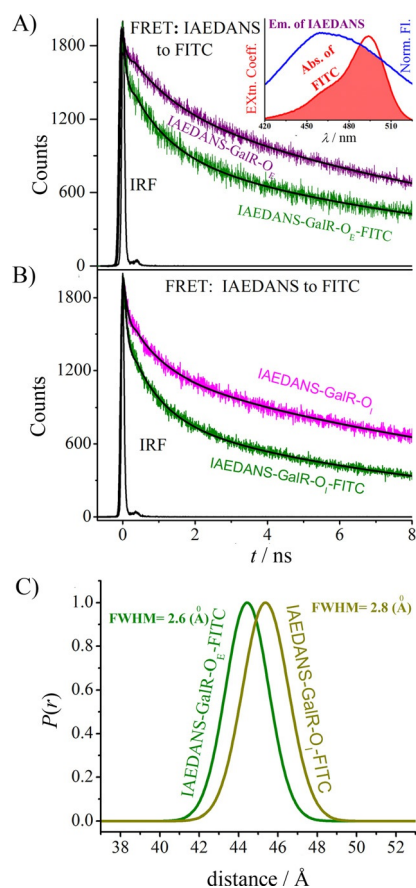


**Figure 6.** Fluorescence transient of IAEDANS–GalR alone or in complex with A) FITC-labelled  $O_E$  or B) FITC-labelled  $O_I$ ;  $\lambda_{\text{ex}} = 375$  nm,  $\lambda_{\text{em}} = 460$  nm. C) Distribution of donor–acceptor distances in complexes with FITC-labelled  $O_E$  and  $O_I$ . IRF: instrument response function.

studies from IAEDANS to FITC attached to the operator (Figure 6A and B). A strong spectral overlap ( $1.32 \times 10^{15} \text{ M}^{-1} \text{ cm}^{-1} \text{ nm}^4$ ) of the emission spectrum of IAEDANS with the absorption spectrum of FITC in  $O_E$  (Figure 6A, inset) reveals the possibility of energy transfer from IAEDANS to FITC. The overlap for the  $O_I$  complex was almost the same ( $1.52 \times 10^{15} \text{ M}^{-1} \text{ cm}^{-1} \text{ nm}^4$ ). A significantly faster transient of 70 ps (45%, at 460 nm) for IAEDANS was evident for the complex with FITC-labelled  $O_E$  compared to the  $O_E$  complex, thus clearly indicating energy transfer from IAEDANS to FITC (Table 4). In the case of the FITC-labelled  $O_I$  complex, the faster component

**Table 4.** Fluorescence lifetimes ( $\tau_i$ ) of IAEDANS attached to a cysteine residue in absence and presence of FITC for different systems.  $\lambda_{\text{ex}} = 375$  nm  $\lambda_{\text{em}} = 460$  nm.

System	$\tau_1$		$\tau_2$		$\tau_3$		$\tau_{\text{avg}}$ [ns]
	[ps]	[%]	[ns]	[%]	[ns]	[%]	
IAEDANS–GalR– $O_E$	260	30	2.80	27	15.90	43	7.70
IAEDANS–GalR– $O_E$ –FITC	70	45	1.05	24	10.00	31	3.45
IAEDANS–GalR– $O_I$	90	42	1.00	21	12.50	37	4.80
IAEDANS–GalR– $O_I$ –FITC	70	55	0.86	21	8.78	24	2.31

was 70 ps (55%). The IAEDANS–FITC distances in repressor– $O_E$ / $O_I$  complexes were 44.1 and 45.5 Å, respectively, and  $R_0$  was 45.97 Å for both systems. It has to be noted that the overall hydrodynamic diameter of GalR is 3.1 nm (Figure 5D), and given linker lengths of 7.4 Å (IAEDANS) and 7.3 Å (FITC), the total distance from IAEDANS to FITC was calculated to be 45.7 Å, which is comparable to our measurements. In our study, small but different FRET distances from IAEDANS to FITC were evident for the two operator–repressor complexes. The difference could be attributable to the different of operators, which induce conformational change in the C terminus, transmitted from N terminus for the two complexes.

Taken together, our results confirm the location of the covalently cysteine-attached IAEDANS as 20.5/20.7 Å from the tryptophan residue and 44.1/45.5 Å from FITC in the operator for GalR– $O_E$ /GalR– $O_I$  complexes. We also calculated the donor IAEDANS–FITC distance distributions for GalR– $O_E$  and GalR– $O_I$  (Figure 6C). The slightly broader distribution for  $O_I$  (FWHM = 2.8 Å) than for  $O_E$  (FWHM = 2.6 Å) can be rationalised in terms of dynamic fluctuations of the repressor. Broadening of donor–acceptor distance can arise from the flexibility of the FITC probe in the operator; this has little relevance for intra-protein dynamics upon complexation. In order to rule out a contribution solely from FITC in the IAEDANS–FITC distribution, we investigated the polarisation-gated fluorescence of FITC upon complexation with GalR (Figure 7). Anisotropy decays of FITC in both  $O_E$  and  $O_I$  (in the absence of GalR) showed restricted dynamics (700–800 ps to 1–1.2 ns) upon complexation with the repressor protein (time constants in Table 5), thus revealing similar protein binding to both DNA operators.

## Conclusions

It is increasingly clear that the DNA sequence acts as an allosteric ligand, in addition to its role as an anchoring point for the transcription factor. In the glucocorticoid receptor system, the DNA sequence affects the conformation and the functional outcome.<sup>[42]</sup> However, not much is known about the role of protein dynamics. One study suggested that dynamics also plays a role in DNA-sequence-dependent allostery in the lambda system.<sup>[18]</sup> Studies of sub-nanosecond dynamics for the interaction of the repressor protein GalR with the operator DNA sequences  $O_E$  and  $O_I$  raise the possibility that key ultrafast timescales of protein fluctuations are involved in the allosteric regulation of protein dimer–dimer interactions. These studies attempt to link structural and dynamical features for allostery-driven tetramerisation for a higher-order nucleoprotein complex that represses transcription of the Gal operon in *E. coli* by involving a DNA loop encompassing the promoter region.

The structural aspects of the protein–DNA complexes were measured by picoseconds-resolved FRET, which probes the distance between two fluorophore and their structural fluctuations. The studies of FRET from Trp165 to IAEDANS at the C terminus of GalR revealed that intra-protein fluctuation upon binding to  $O_I$  is less than for  $O_E$ . However, for FRET between IAEDANS and another extrinsic probe, FITC in the operator DNA, the faster fluctuation was for the GalR– $O_I$  complex. The

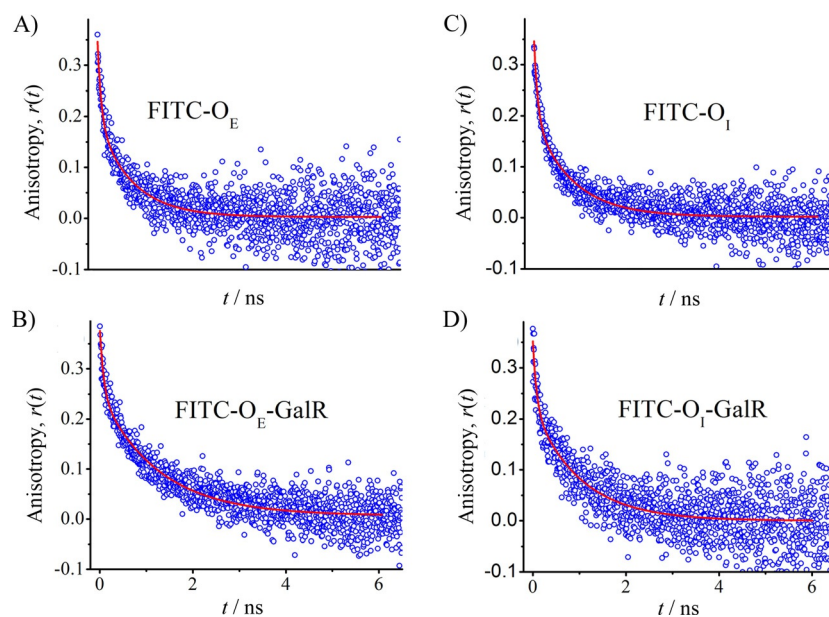


**Figure 7.** Fluorescence anisotropy of FITC in A)  $O_E$ , B) GalR- $O_E$  complex, C)  $O_I$ , and D) GalR- $O_I$  complex. ( $\lambda_{\text{ex}}=445$  nm and  $\lambda_{\text{em}}=520$  nm for all plots.)

System	$\tau_1$		$\tau_2$		$\tau_3$	
	[ps]	[%]	[ns]	[%]	[ns]	[%]
FITC- $O_E$	80	44	0.70	55	30.0	1
FITC- $O_E$ -GalR	80	12	1.20	85	30.0	3
FITC- $O_I$	80	43	0.80	56	30.0	1
FITC- $O_I$ -GalR	80	36	1.00	63	30.0	1

difference in overall protein dynamics upon interaction with DNAs of different sequence is perhaps the key feature in recognising two C-terminal domains during tetramerization of the GalR dimers for its biological function.

The flexibility of the C-terminal domain of GalR was measured by picosecond-resolved polarisation-gated fluorescence spectroscopy, which probes the motion of IAEDANS covalently attached to the active site (C terminus of GalR), far from the effector site (N-terminal). Faster IAEDANS motions were evident upon binding to  $O_I$  than to  $O_E$ . For the lambda repressor, we showed that DNA sequences affect the protein-protein interaction through a distant domain, with concurrent protein dynamics changes.<sup>[18,43]</sup> Whether these two have similar mechanisms is not known, but appears to be likely. Thus differential flexibility at the active site of the protein upon recognition with two different DNA sequences could also be crucial for dimer-dimer interaction through C terminal domains (active sites) for biological function in DNA loop formation in the GalR system. We conclude that the DNA sequence changes subnanosecond motions in a distant site of a transcription factor, and that this likely has functional consequence for the regulation of gene expression. The overall picture that emerges from our studies is depicted in Figure 8.

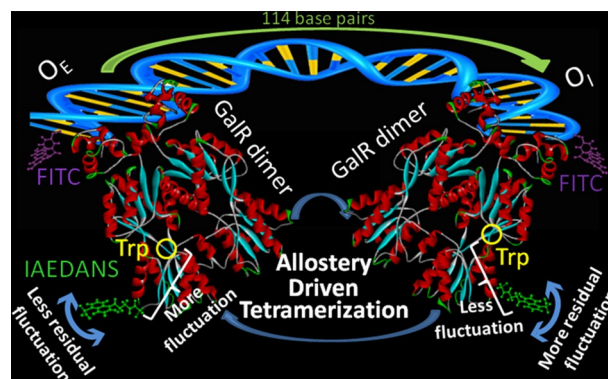


**Figure 8.** Proposed scheme for operator DNA ( $O_E/O_I$ ) bound to GalR dimer undergoing allostery-driven tetramerisation.  $O_E$  induces more protein domain fluctuation compared to  $O_I$ . Flexibility around IAEDANS is more prominent for the  $O_I$ -protein dimer complex than for the  $O_E$  complex.

## Experimental Section

**Chemicals:** 5-(((2-Iodoacetyl)amino)ethyl)amino)naphthalene-1-sulfonic acid (IAEDANS) and fluorescein-5-isothiocyanate (FITC) were purchased from Molecular Probes (ThermoFisher Scientific). Potassium chloride, EDTA, acrylamide, bisacrylamide, TEMED, PMSF, ethidium bromide, Bromophenol Blue, Coomassie Brilliant Blue and ampicillin were from Sigma-Aldrich; anhydrous glycerol was from Merck Millipore. 5'- $C_6$  amino-linked  $O_E$  operator DNA (5'-GCGTG TAAAC GATTC CACGC-3') and its complement, and 5'- $C_6$  amino-linked  $O_I$  (5'-GCGTG GTAGC GGTTA CATGC-3') and its complement were purchased from Trilink Technologies (San Diego, CA). Ni-NTA Sepharose was from GE Healthcare. Lysogeny Broth (LB) and agar powder were from HiMedia (Mumbai, India). Triton X-100 was from MP Biomedicals (Santa Ana, CA). Dipotassium hydrogen phosphate, imidazole, Tris-HCl, NaCl, sodium carbonate and sodium bicarbonate were from J. T. Baker (India). Streptomycin sulfate was from Sigma-Aldrich. L-Arabinose was purchased from Sisco Research Laboratories Pvt. Ltd. (Mumbai, India).

**Protein purification and labelling with IAEDANS:** GalR was expressed from plasmid pSEM1026 and purified as described previously.<sup>[21]</sup> The plasmid was a generous gift from Dr. Sankar Adhya (NIH, Bethesda, MD). GalR is reported to form a stable dimer in aqueous solution, with the C terminus exposed for tetramerisation.

IAEDANS is a thiol-reactive fluorescence probe. At near-neutral (physiological) pH protein can be coupled with thiol groups selectively in the presence of amine groups.<sup>[44]</sup> The site of reaction is an active cysteine in the protein. It has to be noted that all GalR cysteine residues are in the C-terminal domain (active site).<sup>[45]</sup> GalR (11  $\mu\text{M}$ ) and IAEDANS (50  $\mu\text{M}$ ) were incubated in phosphate buffer (0.1 M, pH 8) overnight in the dark and extensively dialysed against the same phosphate buffer before use.

**DNA labelling with FITC:** Operator DNA with a 5'-C6 aminolink was labelled with FITC in sodium carbonate/bicarbonate buffer (500  $\mu\text{L}$ , 1 M, pH 9.0)/DMF/water (5:2:3, v/v/v) by following the procedure published elsewhere.<sup>[46]</sup>

**Experimental details:** All experiments were performed in room temperature ( $\sim 20^\circ\text{C}$ ).

**Absorption and fluorescence study:** Absorbance measurements were performed in a UV-2450 spectrophotometer (Shimadzu). Fluorescence measurements were performed in a Fluoromax-3 fluorimeter (Jobin Yvon Horiba):  $\lambda_{\text{ex}} = 280\text{ nm}$  (tryptophan), 375 nm (IAEDANS); excitation/ emission bandpass 3 nm.

Using the absorption technique reported previously,<sup>[47]</sup> we calculated the labelling efficiency of IAEDANS to GalR and FITC to DNA. Absorbance at 280 nm for the GalR-IAEDANS complex can be expressed as

$$A_{280} = \varepsilon_1 \times c_1 \times l + \varepsilon_2 \times c_2 \times l \quad (1)$$

where  $\varepsilon_1$  and  $\varepsilon_2$  are extinction coefficient at 280 nm (GalR and IAEDANS, respectively),  $c_1$  and  $c_2$  are the concentrations of GalR and IAEDANS, respectively, in the complex,  $l$  is the path length. To determine the concentration of IAEDANS in the complex, we first determined  $\varepsilon$  at 363 nm, where GalR does not absorb.

Absorbance at 363 nm for the GalR-IAEDANS complex is thus,

$$A_{363} = \varepsilon'_1 \times c'_1 \times l'_1 + \varepsilon'_2 \times c'_2 \times l'_2 \quad (2)$$

The extinction coefficient ( $\varepsilon_1$ ) of GalR at 280 nm is  $36900\text{ M}^{-1}\text{ cm}^{-1}$ .<sup>[47]</sup> The extinction coefficient of free IAEDANS in buffer at 337 nm is  $6100\text{ M}^{-1}\text{ cm}^{-1}$ .<sup>[48]</sup> We have calculated the extinction coefficient of free IAEDANS from absorption data to be 2400 and  $4100\text{ M}^{-1}\text{ cm}^{-1}$  at 280 and 363 nm, respectively.

The first part in the right hand side of the Equation (2) is for GalR and will be equal to zero because at 363 nm the absorption is solely due to IAEDANS. Having evaluated  $c_1$ , from Equation (1) we then determined the GalR concentration in the GalR-IAEDANS complex. The ratio of concentration of IAEDANS and GalR yield the labelling efficiency: 82% (0.82 mol IAEDANS for 1 mol GalR monomer). For FITC labelling of operator DNA, we used absorbance values at 260 and 490 nm for DNA and FITC, respectively. This confirmed a FITC/oligomer duplex labelling efficiency of nearly 1.

**Dynamic light-scattering (DLS) study:** DLS measurements were performed with a Zetasizer Nano S instrument (Malvern Instruments, Malvern, UK). Solution in the sample scattered the photon at a fixed wavelength (173 Å). The instrument measures time-dependent fluctuations in the intensity of scattered light. Using the

instrumental software Zetasizer (Malvern Instruments), hydrodynamic diameter ( $d_h$ ) and size distribution of the scatterer in each sample were obtained. In a typical DLS plot, x-axis is hydrodynamic diameter (nanometers) and the y-axis is scattered intensity.

**Time-resolved study:** Time-resolved spectroscopic data were collected by time-correlated single photon counting (TCSPC) with a excitation source of third harmonic laser beam (283 nm) of 850 nm (0.5 nJ per pulse) with instrument response function (IRF) of 50 ps to excite tryptophan residue; details of the instrument can be found elsewhere.<sup>[40]</sup> For the excitation of IAEDANS and FITC probes we used a LifeSpec-ps picosecond diode laser-pumped fluorescence spectrophotometer from Edinburgh Instruments (Livingston, U.K). Picosecond excitation pulses from the picoquant diode laser were used at 375 nm and 445 nm with an IRF of 50 ps. A microchannel-plate-photomultiplier tube (MCP-PMT; Hamamatsu Photonics, Kyoto, Japan) was used to detect the photoluminescence from the sample after dispersion through a monochromator. The observed fluorescence transients were fitted by using a nonlinear least-square fitting procedure to a function with software F900 from Edinburgh Instruments (Livingston, U.K).

The quality of the curve fitting was evaluated by reduced chi-square and residual data. It has to be noted that with our time-resolved instrument, we can resolve at least one fifth of the instrument response time constants after the de-convolution of the IRF. The average lifetime (amplitude-weighted) of a multi-exponential decay is expressed as:

$$\tau_{\text{av}} = \sum_{i=1}^N c_i \tau_i$$

For anisotropy measurement we collected fluorescence transients with the emission polariser parallel to and perpendicular to that of the excitation. Anisotropy ( $r(t)$ ) was obtained by following the equation,

$$r(t) = \frac{I_{\text{para}} - G \times I_{\text{perp}}}{I_{\text{para}} + 2 \times G \times I_{\text{perp}}}$$

where  $I_{\text{para}}$  and  $I_{\text{perp}}$  are fluorescence emission keeping polariser at parallel and perpendicular to that of the excitation respectively.  $G$  is the grating factor.

**FRET study:** FRET distances were calculated from the lifetime transients of donor and acceptor, obtained from LifeSpec-ps instrument. Donor-acceptor distance ( $r$ ) was calculated from the equation:

$$r^6 = [R_0^6(1-E)]/E$$

where  $R_0$  is the Förster distance, and  $E$  is the efficiency of the energy transfer between donor-acceptor.  $E$  was calculated using the equation

$$E = 1 - \frac{\tau_{\text{DA}}}{\tau_{\text{D}}}$$

where  $\tau_{\text{DA}}$  and  $\tau_{\text{D}}$  are fluorescence lifetimes of the donor in presence and absence of acceptor.

The Förster distance ( $R_0$  [Å]) was calculated from the overlap integral of the emission spectrum of the donor and absorption spectrum of the acceptor from the equation

$$R_0 = 0.211 \times [\kappa^2 \eta^{-4} \Phi_D J(\lambda)]^{1/6}$$

where  $\kappa^2$  is a factor describing the relative orientation in space of the transition dipoles of the donor and the acceptor. The magnitude of  $\kappa^2$  is assumed to be 0.66 for random orientation of the donor and the acceptor. The refractive index ( $\eta$ ) of the biological medium is assumed to be 1.4.<sup>[30]</sup>  $J(\lambda)$  is the overlap integral of emission of donor and absorption of acceptor and calculated by

$$J(\lambda) = \frac{\int_0^\infty F_D(\lambda) \varepsilon(\lambda) \lambda^4 d\lambda}{\int_0^\infty F_D(\lambda) d\lambda}$$

where  $F_D(\lambda) d\lambda$  is the fluorescence emission of the donor in the wavelength region  $\lambda$  to  $\lambda+d\lambda$ .  $\varepsilon(\lambda)$  is extinction coefficient [ $\text{M}^{-1} \text{cm}^{-1}$ ] of acceptor.

**FRET distance distribution calculation:** Distance distribution function  $P(r)$  was evaluated using the procedure described in the previous literature.<sup>[30,49,50]</sup> The decay transient of donor in absence of acceptor were fitted using nonlinear least-squares fitting procedure (software SCIENTIST from Micromath (Saint Louis, MO, USA)) to the following function

$$I_D(t) = \int_0^t E(t) P(t-t) dt'$$

which comprises the convolution of the IRF( $E(t)$ ) with exponential

$$P(t) = \sum \alpha_{Di} \exp(-t/\tau_{Di})$$

The distance distribution function  $P(r)$  in the fluorescence transients of donor in presence of acceptor in the systems under study is calculated using the same software in the following way.

The intensity decay of donor–acceptor pair spaced at a distance  $r$  is given by

$$I_{DA}(r,t) = \sum \alpha_{Di} \exp\left[-\frac{t}{\tau_{Di}} - \frac{t}{\tau_D} \left(\frac{R_0}{r}\right)^6\right]$$

and the intensity decay of the sample considering  $P(r)$  is given by

$$I_{DA}(t) = \int_{r=0}^\infty P(r) I_{DA}(r,t) dr$$

where

$$P(r) = \frac{1}{\sigma\sqrt{2\pi}} \exp\left[-\frac{1}{2} \left(\frac{\bar{r}-r}{\sigma}\right)^2\right]$$

where  $\bar{r}$  is the mean of the Gaussian with a standard deviation of  $\sigma$  and  $r$  is the donor–acceptor distance. The distance distribution are described by full width at half maxima (FWHM) =  $2.354\sigma$ . We have calculated the resolution of our distance distribution is 0.1 Å given the resolution of the time resolved measurements to be 10 ps.

## Acknowledgements

The plasmid used during protein purification was a generous gift from Dr. Sankar Adhya's laboratory (NIH, Bethesda, MD 20892-4264, USA). S.C. thanks the CSIR, India for the research fellowships. We thank DST (India) for financial grants (SB/S1/PC-011/2013 and DST/TM/SERI/2k11/103) and DAE (India) for (2013/37P/73/BRNS). PL thanks the NTH-School "Contacts in Nanosystems: Interactions, Control and Quantum Dynamics", the Braunschweig International Graduate School of Metrology, and DFG-RTG 1952/1, Metrology for Complex Nanosystems.

**Keywords:** allostery • conformational dynamics • FRET • gene expression • operator DNA • protein structures

- [1] A. Manglik, B. Kobilka, *Curr. Opin. Cell Biol.* **2014**, *27*, 136–143.
- [2] W. A. Eaton, V. Muñoz, S. J. Hagen, G. S. Jas, L. J. Lapidus, E. R. Henry, J. Hofrichter, *Annu. Rev. Biophys. Biomol. Struct.* **2000**, *29*, 327–359.
- [3] M. Karplus, J. Kuriyan, *Proc. Natl. Acad. Sci. USA* **2005**, *102*, 6679–6685.
- [4] H. Frauenfelder, B. H. McMahon, R. H. Austin, K. Chu, J. T. Groves, *Proc. Natl. Acad. Sci. USA* **2001**, *98*, 2370–2374.
- [5] J. Monod, J. Wyman, J.-P. Changeux, *J. Mol. Biol.* **1965**, *12*, 88–118.
- [6] H. N. Motlagh, J. O. Wrabl, J. Li, V. J. Hilser, *Nature* **2014**, *508*, 331–339.
- [7] S.-R. Tzeng, C. G. Kalodimos, *Nature* **2009**, *462*, 368–372.
- [8] J.-P. Changeux, S. J. Edelstein, *Science* **2005**, *308*, 1424–1428.
- [9] N. Popovych, S. Sun, R. H. Ebright, C. G. Kalodimos, *Nat. Struct. Mol. Biol.* **2006**, *13*, 831–838.
- [10] C.-J. Tsai, A. del Sol, R. Nussinov, *J. Mol. Biol.* **2008**, *378*, 1–11.
- [11] V. J. Hilser, J. O. Wrabl, H. N. Motlagh, *Annu. Rev. Biophys.* **2012**, *41*, 585–609.
- [12] T. C. B. McLeish, T. L. Rodgers, M. R. Wilson, *Phys. Biol.* **2013**, *10*, 056004.
- [13] A. Cooper, D. T. F. Dryden, *Eur. Biophys. J.* **1984**, *11*, 103–109.
- [14] H.-S. Won, T. Yamazaki, T.-W. Lee, M.-K. Yoon, S.-H. Park, Y. Kyogoku, B.-J. Lee, *Biochemistry* **2000**, *39*, 13953–13962.
- [15] R. A. Laskowski, F. Gerick, J. M. Thornton, *FEBS Lett.* **2009**, *583*, 1692–1698.
- [16] S. Choudhury, S. Batabyal, P. K. Mondal, P. Singh, P. Lemmens, S. K. Pal, *Chem. Eur. J.* **2015**, *21*, 16172–16177.
- [17] J. Kuriyan, D. Eisenberg, *Nature* **2007**, *450*, 983–990.
- [18] T. Mondol, S. Batabyal, A. Mazumder, S. Roy, S. K. Pal, *FEBS Lett.* **2012**, *586*, 258–262.
- [19] A. Majumdar, S. Adhya, *J. Biol. Chem.* **1987**, *262*, 13258–13262.
- [20] A. Majumdar, S. Adhya, *Proc. Natl. Acad. Sci. USA* **1984**, *81*, 6100–6104.
- [21] S. Semsey, M. Geanacopoulos, D. E. A. Lewis, S. Adhya, *EMBO J.* **2002**, *21*, 4349–4356.
- [22] S. Batabyal, S. Choudhury, D. Sao, T. Mondol, S. Kumar Pal, *Biomol. Concepts* **2014**, *5*, 21–43.
- [23] M. Brenowitz, E. Jamison, A. Majumdar, S. Adhya, *Biochemistry* **1990**, *29*, 3374–3383.
- [24] S. E. Bondos, L. Swint-Kruse, K. S. Matthews, *J. Biol. Chem.* **2015**, *290*, 24669–24677.
- [25] C. Zwiebe, J. Kim, S. Adhya, *Genes Dev.* **1989**, *3*, 606–611.
- [26] B. von Wilcken-Bergmann, B. Müller-Hill, *Proc. Natl. Acad. Sci. USA* **1982**, *79*, 2427–2431.
- [27] J. Yang, Y. Zhang, *Nucleic Acids Res.* **2015**, *43*, W174–W181.
- [28] L. Swint-Kruse, K. S. Matthews, *Curr. Opin. Microbiol.* **2009**, *12*, 129–137.
- [29] S. Nag, B. Sarkar, M. Chandrakesan, R. Abhyanakar, D. Bhowmik, M. Kombrabail, S. Dandekar, E. Lerner, E. Haas, S. Maiti, *Phys. Chem. Chem. Phys.* **2013**, *15*, 19129–19133.
- [30] J. R. Lakowicz, *Principles of Fluorescence Spectroscopy*, 3rd ed., Springer, **2013**.
- [31] S. S. Lehrer, *Biochemistry* **1971**, *10*, 3254–3263.
- [32] D. Kern, E. R. P. Zunderweg, *Curr. Opin. Struct. Biol.* **2003**, *13*, 748–757.
- [33] G. Li, D. Magana, R. B. Dyer, *Nat. Commun.* **2014**, *5*, 3100.
- [34] A. J. Wand, *Curr. Opin. Struct. Biol.* **2013**, *23*, 75–81.
- [35] H.-X. Zhou, M. K. Gilson, *Chem. Rev.* **2009**, *109*, 4092–4107.

- [36] M. S. Marlow, J. Dogan, K. K. Frederick, K. G. Valentine, A. J. Wand, *Nat. Chem. Biol.* **2010**, *6*, 352–358.
- [37] J. A. McCammon, B. R. Gelin, M. Karplus, *Nature* **1977**, *267*, 585–590.
- [38] F. R. N. Gurd, T. M. Rothgeb, *Adv. Protein Chem.* **1979**, *33*, 73–165.
- [39] S. Choudhury, S. Batabyal, T. Mondol, D. Sao, P. Lemmens, S. K. Pal, *Chem. Asian J.* **2014**, *9*, 1395–1402.
- [40] T. Mondol, S. Batabyal, S. K. Pal, *J. Biomol. Struct. Dyn.* **2012**, *30*, 362–370.
- [41] K. K. Frederick, M. S. Marlow, K. G. Valentine, A. J. Wand, *Nature* **2007**, *448*, 325–329.
- [42] S. H. Meijssing, M. A. Pufall, A. Y. So, D. L. Bates, L. Chen, K. R. Yamamoto, *Science* **2009**, *324*, 407–410.
- [43] S. Deb, S. Bandyopadhyay, S. Roy, *Biochemistry* **2000**, *39*, 3377–3383.
- [44] G. T. Hermanson, *Bioconjugate Techniques* (3rd ed.), Academic Press, **2013**.
- [45] D. Ajdić, J. J. Ferretti, *J. Bacteriol.* **1998**, *180*, 5727–5732.
- [46] A. Maiti, S. Roy, *Nucleic Acids Res.* **2005**, *33*, 5896–5903.
- [47] S. Chatterjee, Y.-N. Zhou, S. Roy, S. Adhya, *Proc. Natl. Acad. Sci. USA* **1997**, *94*, 2957–2962.
- [48] G. Haran, E. Haas, B. K. Szpikowska, M. T. Mas, *Proc. Natl. Acad. Sci. USA* **1992**, *89*, 11764–11768.
- [49] S. Choudhury, P. K. Mondal, V. K. Sharma, S. Mitra, V. G. Sakai, R. Mukhopadhyay, S. K. Pal, *J. Phys. Chem. B* **2015**, *119*, 10849–10857.
- [50] S. Batabyal, T. Mondol, S. Choudhury, A. Mazumder, S. K. Pal, *Biochimie* **2013**, *95*, 2168–2176.

---

Manuscript received: December 9, 2015

Accepted article published: February 23, 2016

Final article published: March 3, 2016

---